This is a preprint; final revised version published as
Colloids Surf. A Physicochem. Eng. Asp. **629** (2021) 127414.
DOI: 10.1016/j.colsurfa.2021.127414

The cause of accelerated desorption of sparingly soluble dodecanol monolayers: convection or leakage?

Ivan L. Minkov,*[,a,b] Iglika M. Dimitrova,[c,d] Dimitrinka Arabadzhieva,[b] Elena Mileva,[b] Radomir I. Slavchov[e]

[a] *Department of Chemistry and Biochemistry, Physiology, and Pathophysiology, Faculty of Medicine, Sofia University, 1 Koziak Str., 1407 Sofia, Bulgaria*
[b] *Bulgarian Academy of Sciences, Institute of Physical Chemistry "Rostislaw Kaischew", Akad. G. Bonchev Str., bl.11, 1113 Sofia, Bulgaria, Sofia, Bulgaria*
[c] *Department of Physical Chemistry, Faculty of Chemical Technologies, University of Chemical Technology and Metallurgy, 8 Kl. Ohridski Blvd., 1756 Sofia, Bulgaria*
[d] *Institute of Solid State Physics, Bulgarian Academy of Sciences, 72 Tzarigradsko Chaussee Blvd., BG-1784 Sofia, Bulgaria*
[e] *School of Engineering and Materials Science, Queen Mary University of London, Mile End Road, London E1 4NS, United Kingdom*
**E-mail:* i_minkov@chem.uni-sofia.bg

Abstract. The dissolution of sparingly soluble surfactants from spread monolayers is a complex multi-staged process. The desorption of dodecanol from the surface of water follows mixed barrier/diffusion kinetics only in the first stages of the dissolution. Significant acceleration of the desorption has been observed experimentally after this initial period, which has been hypothesized to be due to onset of convective diffusion; the source of convection, however, has not been identified. The goal of this work was to investigate the question through desorption experiments under controlled convection and respective modelling of the process under mixed barrier/convective diffusion control. Several hypotheses for the cause of the accelerated desorption were tested. The analysis shows that natural convection, Marangoni convection, convection due to the motion of the barrier of the Langmuir trough, and artificial convection caused by an electromagnetic stirrer cannot produce desorption rates of the observed magnitude. The most likely reason for the acceleration is identified as leakage through the barrier. The rate of this leakage is estimated form the experimental data.

Keywords: kinetics of adsorption-desorption, barrier for desorption, convective diffusion, Langmuir trough, leakage through the barrier

1. Introduction

The rate of adsorption or desorption of surfactants affects many natural and industrial processes: emulsification [1-3], corrosion inhibition [4,5], and others. The kinetics of adsorption-desorption is usually studied with monolayers of constant area, by monitoring the change of surface tension σ with time t [6,7,8-12]. An alternative approach is desorption of spread sparingly soluble monolayer under *2D-isobaric mode* of operation of the Langmuir trough, where the area A of the contracting monolayer is followed with t under constant σ [13-21]. The advantage of this technique is that the adsorption Γ and the desorption rate (which is a strong function of Γ [22]) do not change during the dissolution. The isobaric experiment simplifies data processing compared to constant area conditions. It also allows for better control of the convective transport of surfactant [23-25], which is important from practical standpoint as vigorous mixing is common in most industrially relevant applications of surfactants.

The process of dissolution of sparingly soluble surfactant monolayers under 2D-isobaric conditions has been reported to proceed in several stages [22,23,24]. At short times, the rate-determining step of the process is the so-called barrier (flip-flop) desorption. It corresponds to area of the monolayer A decreasing exponentially with time, i.e. $\ln(A_0/A) \propto t$ (where A_0 is the initial area of the monolayer). The coefficient of proportionality is related to the energetic barrier for transfer of a molecule from the monolayer to the subsurface. The experimental data for this regime allows the mean time τ_d that a molecule spends at the surface to be determined [22]. The barrier control is typical for desorption of bulky adsorbates such as proteins, aggregates, nanoparticles etc. [26], but the process is *always* under barrier control at times small enough ($t < \tau_d$), even for molecules of small molecular weight [22,26].

In the absence of convection, a second, diffusion-controlled stage follows. In this regime, the area of the monolayer follows a logarithmic-parabolic kinetics, $\ln(A_0/A) \propto t^{1/2}$, and the parameter that controls the rate is the bulk diffusion coefficient D of the surfactant in the solution. Under this regime, the thickness of the surfactant-saturated subsurface (*the diffusion layer*) increases proportionally to $t^{1/2}$.

When the diffusion layer becomes thick enough, the inevitable convection in the substrate speeds up the diffusion process and the system enters a third, convective diffusion regime, demonstrated long ago by Ter Minassian-Saraga [23,24].

The phenomenon that we study in the current work is the increased rate of desorption from a spread monolayer from the surface of a Langmuir trough in comparison with the classic barrier-diffusion regime. The phenomenon is illustrated in Figure 1. Sparingly soluble dodecanol monolayer is spread on a surface and quickly shrunk to a predetermined surface pressure ($\pi^S \equiv \sigma_0 - \sigma = 5$ mN/m, where σ_0 is pure water's surface tension). The barostat is then switched on – the Langmuir trough compensates for the dissolution of material by shrinking the monolayer via two movable Teflon barriers, until $\pi^S = 5$ mN/m is restored. As the monolayer dissolves, the area occupied by it decreases; the drop in area is a direct measure for the loss of material. For small times, the data in Figure 1 follow mixed barrier-diffusion mode of desorption [26,27]; this time interval has been studied previously [22,28]. However, very often and especially at increased

temperature, we see significant deviation from the theoretically expected behaviour corresponding to acceleration of desorption after the initial period (illustrated with an arrow in Figure 1). The deviation was hypothesized to be due to convective flows in the aqueous substrate, leading to barrier/convective diffusion regime of desorption. As per our hypothesis, vigorous convection should result in fast transport and rate-determining barrier desorption, i.e. energetic mixing means barrier control; indeed, especially at increased temperature, we do observe linear isobars ln$A(t)$, as if desorption is under barrier control [22].

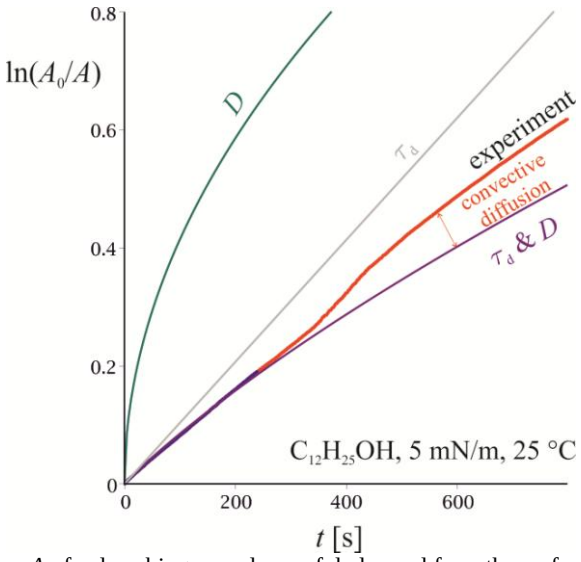

Figure 1. Decrease of the area A of a desorbing monolayer of dodecanol from the surface of water at a fixed surface pressure $\pi^S = 5$ mN/m, in coordinates A/A_0 vs. time t. The deviation between the experimental results and the theoretically predicted 2D-isobar under mixed barrier-diffusion control (curve τ_d & D) has been previously ascribed to unspecified source of convection.

Our previous study was inconclusive as it was unclear from our experiments what could be the source of the hypothetical convection. Here, we set the goal to examine theoretically and experimentally several hypotheses about the origin of the accelerated desorption rate:

(i) The convection is natural, a result of temperature gradients in the aqueous substrate, causing corresponding density gradients [29].

(ii) The convection is caused by the movement of the Teflon barrier of the Langmuir trough (hypothesis expressed and analyzed by de Keiser and Joos [25]).

(iii) The convection is caused by Marangoni effects due to surface temperature gradients [31], or to Gibbs-Marangoni effect caused by readsorption behind the barriers.

(iv) The observed acceleration is not caused by convection, but by material loss as result of diffusion trough the barrier [32, 33, 34].

As part of our experimental analysis, we studied desorption for prolonged periods of time, with substrates of different depth, and with forced acceleration of the convective transport. Under such conditions, the monolayer can saturate the substrate to a significant degree, i.e. the concentration of surfactant in the substrate increases with time to non-negligible values, diminishing the dissolution rate. In order to obtain quantitative results for the rate of desorption, this saturation effect has to be accounted for. We did so by generalizing the theory of isobaric desorption to substrates of non-infinite thickness.

2. Theoretical part

The theory of desorption under isobaric regime for the case of mixed convective diffusion-barrier control was developed by Patlak and Gershfeld [27] and Baret et al. [26]. Here, we modify it to take into account the saturation of the substrate. According to the results from Ref. [26,27], the initial stage of the dissolution is non-stationary, with diffusion layer of thickness $\sim(Dt)^{1/2}$ that increases with time. In the absence of convection, Fick's second law reads

$$\frac{\partial C}{\partial t} = -\frac{\partial j_D}{\partial z} = D\frac{\partial^2 C}{\partial z^2}\,. \tag{1}$$

Here, the phenomenological relationship $j_D = -D\partial C/\partial z$ is assumed to hold for the diffusion flux. The barrier desorption process has to be accounted for through another phenomenological law for the flux j^S of molecules desorbing from the surface. Following Ref. [26,27], we assume that it is proportional to the difference between the concentration C_{eq} of substrate in equilibrium with the monolayer (fixed by the adsorption isotherm) and the actual surfactant concentration $C(z = 0)$ right next to the surface:

$$j^S = k_d\left[C_{eq} - C\left(z=0,t\right)\right] = \frac{\Gamma}{\tau_d}\left[1 - \frac{C\left(z=0,t\right)}{C_{eq}}\right], \tag{2}$$

where k_d is the rate constant of the desorption process of rate $v_d = k_d C_{eq}$ (see Figure 2); k_d is a function of the temperature and the density Γ of the monolayer. We introduced the characteristic time τ_d for desorption of a surfactant molecule at the surface (mean residence time of an adsorbed molecule in a monolayer of fixed density), which is related to k_d as

$$\tau_d = \Gamma / k_d C_{eq}\,. \tag{3}$$

Case 1: no convection, no saturation. For infinitely thick substrate, the boundary and initial conditions on $C(z,t)$ read:

$$D\left.\frac{\partial C}{\partial z}\right|_{z=0} = j^S; \qquad C\left(z=-\infty,t\right)=0; \qquad C\left(z,t=0\right)=0\,. \tag{4}$$

In the case of fast desorption, τ_d is a small parameter, k_d is a large, and Eqs. (2)&(4) simplify to the usual condition for saturated subsurface, $C(z = 0) = C_{eq}$. For long desorption times τ_d, $C(z = 0)$ can differ significantly from C_{eq}. The solution to Eqs. (1), (2) and (4) is known [26,27]; the result for the desorption flux j^S of surfactant from the surface is:

$$j^S = \frac{\Gamma}{\tau_d}\mathrm{e}^{t/\tau_{tr}}\left(1 - \mathrm{erf}\sqrt{t/\tau_{tr}}\right), \tag{5}$$

where τ_{tr} is a characteristic time for transition from barrier regime to mixed barrier/diffusion regime, defined as

$$\tau_{tr} = DC_{eq}^2\tau_d^2/\Gamma^2\,. \tag{6}$$

The result is easily generalized to the case where there is a non-zero bulk concentration of surfactant, so the boundary condition $C(-\infty,t) = C_\infty$ holds instead of Eq. (4):

$$j^{\mathrm{S}} = \frac{\Gamma}{\tau_{\mathrm{d}}}\left(1-\frac{C_\infty}{C_{\mathrm{eq}}}\right)\mathrm{e}^{t/\tau_{\mathrm{tr}}}\left(1-\mathrm{erf}\sqrt{t/\tau_{\mathrm{tr}}}\right). \qquad (7)$$

The time integral of the flux j^{S} gives the total material that leaves the surface. This is what the curve "mixed barrier/diffusion regime" in Figure 1 stands for. We have applied this result [22,28] to data for the initial stage of desorption of dodecanol before the hypothetical convection starts playing any role in the dissolution. The coefficient k_{d} and the desorption time τ_{d} were determined by fitting desorption isobars such as the one presented in Figure 1; the diffusion coefficient was determined independently.

Case 2: desorption with convection, no saturation. For the case of *barrier desorption+convective diffusion*, one can use the stagnated layer model [24,26] (see Figure 2). It assumes that the substrate consists of two distinct layers of fluid: right next to the immobile surface, the fluid is immobilized and the convection has no effect on the transport rate (the *stagnated layer* of thickness L_{st}); below the stagnated layer, the convection is intensive enough to homogenize the concentration in the liquid. In other words the diffusion process is taking place within a layer $0 < z < -L_{\mathrm{st}}$. At $z < -L_{\mathrm{st}}$, the concentration C_∞ is equal everywhere in the bulk solution due to the convection. The length L_{st} depends on the convection source and the geometrical parameters of the flow; intensive convection means low L_{st}, and L_{st} is related to the shear rate as $L_{\mathrm{st}} \propto D^{1/2}(\mathrm{d}v_x/\mathrm{d}z)^{-1/2}$.

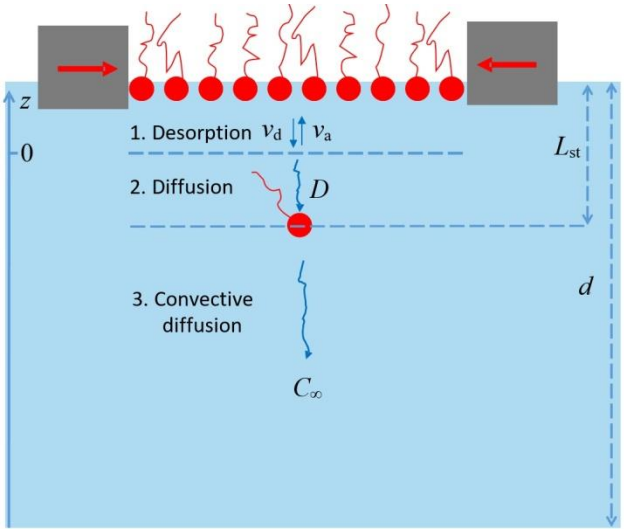

Figure 2. Schematic representation of the stagnated layer model.

Thus, the stagnated layer model corresponds to boundary and initial condition $C(z = -L_{\mathrm{st}}) = C(t = 0) = C_\infty$, cf. Eq. (4). This problem was analysed by Patlak and Gershfeld [27], who obtained for the surface flux the formula

$$j^{\mathrm{S}} = \frac{D}{L_{\mathrm{st}}}\left(C_{\mathrm{eq}} - C_\infty\right)\left[\frac{M}{1+M} + 2M^2\sum_{n=1}^{\infty}\frac{\exp\left(-m_n^2 t/\tau_{\mathrm{st}}\right)}{M + M^2 + m_n^2}\right], \qquad (8)$$

where the dimensionless number M is a ratio between the flip-flop desorption and diffusion fluxes:

$$M = L_{\mathrm{st}}\Gamma/\tau_{\mathrm{d}}C_{\mathrm{eq}}D, \qquad (9)$$

and the coefficients m_n are the zeros of the equation

$$m\cot(m)+M=0. \tag{10}$$

The characteristic time τ_{st} in Eq. (8) is for transition from *barrier/diffusion* to *barrier/convective diffusion* regime, and is defined as

$$\tau_{st}=L_{st}^2/D\ . \tag{11}$$

At times $t<\tau_{st}$ the barrier/diffusion regime of dissolution and Eq. (7) holds, while at $t>\tau_{st}$ the convection starts to play substantial role. At $t>>\tau_{st}$, steady state is approached, where the surface flux of surfactant is given by

$$j_\infty^S=\frac{D}{L_{st}}\frac{M}{1+M}\left(C_{eq}-C_\infty\right). \tag{12}$$

For constant bulk concentration C_∞, the steady flux j_∞^S is constant and the dependence of $\ln(A/A_0)$ on t is linear.

Case 3: desorption with convection and saturation. We now consider the case where C_∞ changes with time, due to saturation of the substrate by the dissolving monolayer. To solve this problem, we will observe that the depth d of the substrate (~cm) is normally significantly thicker than the stagnated layer thickness L_{st} (~0.1 mm), which means that by the time saturation starts to play a role, the steady state in the stagnated layer is already established, i.e. Eq. (12) is valid. In this approximation, C_∞ can be determined from a simplified mole balance

$$Ad\frac{\mathrm{d}C_\infty}{\mathrm{d}t}=Aj_\infty^S,\quad \text{i.e.}\quad \frac{\mathrm{d}C_\infty}{\mathrm{d}t}=\frac{j_\infty^S}{d}. \tag{13}$$

The diffusion through the side perimeter of the volume Ad is ignored; j_∞^S is given by Eq. (12) but with time-dependent $C_\infty(t)$ (quasi-steady state approximation). The solution to Eq. (13) with initial condition $C_\infty(t=0)=0$ is

$$C_\infty(t)=C_{eq}\left(1-\mathrm{e}^{-\frac{M}{1+M}\frac{t}{\tau_{sat}}}\right), \tag{14}$$

where

$$\tau_{sat}=L_{st}d/D \tag{15}$$

is a characteristic time for saturation, which defines when the confinement from the depth of the aqueous substrate starts playing a role. Since the depth of the stagnated layer is much smaller than the depth of the substrate, $L_{st}<<d$, it holds true that $\tau_{st}<<\tau_{sat}$ (compare Eq. (11) and (15)). The surface flux corresponding to Eq. (14) is given by

$$j_\infty^S=\frac{D}{L_{st}}\frac{M}{1+M}\left(C_{eq}-C_\infty(t)\right)=\frac{DC_{eq}}{L_{st}}\frac{M}{1+M}\exp\left(-\frac{M}{1+M}\frac{t}{\tau_{sat}}\right). \tag{16}$$

Eq. (16) is valid at times $t>>\tau_{st}$, when the steady state in the stagnated layer has been established ($j^S\xrightarrow{t\gg\tau_{st}}j_\infty^S$). On the other hand, the non-steady state solution (8) that ignores the saturation is valid for $t<<\tau_{sat}$. Since $\tau_{st}<<\tau_{sat}$, there exist an intermediate time period, $\tau_{st}<<t<<\tau_{sat}$, where the difference between Eq. (8) and Eq. (16) is negligible (flux is already steady but saturation is still negligible). This allows one to match the two formulae to obtain a flux formula valid at any time:

$$j^{\mathrm{S}} = \frac{D}{L_{\mathrm{st}}} C_{\mathrm{eq}} \left[\frac{M}{1+M} + 2M^2 \sum_{n=1}^{\infty} \frac{\exp\left(-m_n^2 t / \tau_{\mathrm{st}}\right)}{M + M^2 + m_n^2} \right] \exp\left(-\frac{M}{1+M} \frac{t}{\tau_{\mathrm{sat}}} \right) . \qquad (17)$$

The measured quantity is the dependence of the area of the monolayer on time $A(t)$; it follows from the mole balance

$$\frac{1}{A}\frac{\mathrm{d}n}{\mathrm{d}t} = \frac{\Gamma}{A}\frac{\mathrm{d}A}{\mathrm{d}t} = -j^{\mathrm{S}} . \qquad (18)$$

In Eq. (18), we used that $n = \Gamma A$ and that $\Gamma = const$ under isobaric conditions. The integration of eq. (18) is analytic and the result is given in the Suppl. Mat.

Case 4: leakage behind the movable barrier. Let us consider the possibility for some amount of surfactant to leak behind the Teflon barriers to the free surface. This leakage can happen either through tiny fluid channels between the movable barrier and the Teflon trough well, or via surface diffusion through the solid|liquid interface. We modify the mole balance (18) for the surfactant in the monolayer by adding a leak flux:

$$\Gamma \frac{\mathrm{d}A(t)}{\mathrm{d}t} = -j_{\infty}^{\mathrm{S}}(t) A(t) - 2L_{\mathrm{side}} j_{\mathrm{side}} , \qquad (19)$$

where $2L_{\mathrm{side}}$ is the length of the two barriers and $j_{\mathrm{side}} = k_{\mathrm{side}}(\Gamma - \Gamma_{\mathrm{free\ surface}})$ is the flux through the barrier in [mol·s^{-1}·m^{-1}]. In Eq. (19) we have assumed that the steady state is reached so the dissolution flux j_{∞}^{S} is given by Eq. (16). At least for the case where the leakage is slow and $\Gamma_{\mathrm{free\ surface}} << \Gamma$, the integration is again analytic – the result for $A(t)$ is given in Suppl. Mat.

3. Experimental test of the hypotheses

Four types of experiments were performed to test the four hypotheses formulated in the introduction.

Prolonged dissolution. Compared to our previous experiments [22,28], where we monitored the area of the monolayer for a few minutes, in this study, we did experiments continuing for more than an hour, to make sure that the regime controlled by hypothetical convective diffusion was established. The interpretation of these data is complicated by the saturation of the substrate, as discussed in the previous section.

Desorption rate under diminished natural convection. The intensity of natural convection depends strongly on the depth d of the substrate [29]. Were the accelerated desorption caused by natural convection, the desorption rate would diminish at small d. To test this hypothesis, we attached a set of plexiglass plates of varying thickness to the bottom of the Teflon trough. The plate edges were shaped so that they follow tightly the profile of the trough. The plates were pressed against the bottom via specially designed mechanical holders. This ensured reproducible and even reduction in the depth of the trough. The meniscus protrusion above the trough top edge was kept at a level between 0.5 and 2 mm; the depth d includes this protrusion. Using plates with different thickness and heights of the water meniscus, we conducted experiments at depth of the aqueous substrate in the range d = 1-6 mm.

Test of the effect of the Marangoni convection induced by lateral temperature gradient. To test this hypothesis, we performed experiments where a lateral temperature gradient was artificially induced and maintained along the length and width of the Teflon

trough. A directional heat source (an incandescent 7 W bulb) was placed at one side of the trough, 5-6 cm away from the water surface. After filling the trough and before placing the monolayer, the heater was switched on. After 10 min, stationary temperature gradient of about 4 °C along the long axis of the trough was established, and approximately 1 °C from the centre to the edge, along the short axis of the trough. This gradient should be sufficient to produce Marangoni convection, especially in the sector of the trough where no surfactant is spread and the liquid surface is mobile. Acceleration of the natural convection can also be expected.

Test of the effect of mechanical convection. To test whether the observed acceleration of the desorption is due to convection at all, we performed experiments where the water volume was vigorously stirred using two symmetrically arranged magnetic stirrers along the longitudinal axis of the trough. This stirring caused intense convection visible with naked eye in the water volume throughout the experiment.

Test of the Marangoni convection induced by readsorption of the surfactant in the side compartments of the trough, and tests for leakages below the movable barrier. We first did an attempt to measure directly the surface tension in the monolayer-free compartment of the trough after dodecanol is spread in the central compartment (similarly to the monitoring done in Ref. [32]). Leakage and readsorption should lead to decrease in surface tension of the free surface. Next, we did experiments where a dodecanol monolayer was spread on the free surface behind the barriers prior to the experiment (Figure 3). The dodecanol monolayer diminishes the chemical potential and surface tension differences on the two sides of the barrier, which should diminish the driving forces for the transport through the barrier. In some experiments, we tried to use completely insoluble octadecanol monolayer instead of the sparingly soluble dodecanol, in order to additionally restrict the transport back and forth through the barrier (Figure 3).

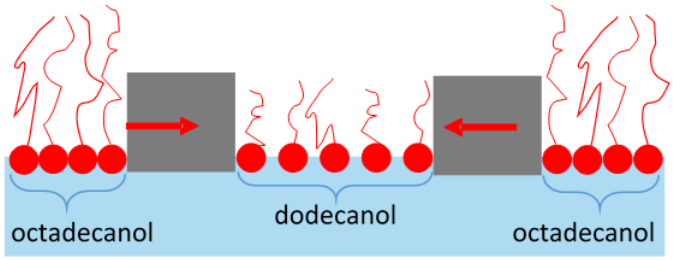

Figure 3. Experiment with octadecanol placed behind the two barriers. Experiments were done also with dodecanol placed behind the barriers.

4. Results and processing/discussion

The original model (8) of Patlak and Gershfeld [27] for surfactant desorption under barrier/convective diffusion control does not compare well with our data for prolonged desorption, see Figure 4(a). We ascribe this to the effect of saturation; indeed, when the increase of C_∞ with time is taken into account, the model and the data agree very well to the point of complete dissolution of the monolayer, see Figure 4(b). The same two adjustable parameters, τ_d and L_{st}, were used for the two regressions; for the diffusion coefficient of dodecanol in water, we used the value $D = 5.15\times10^{-10}$ m^2 s^{-1}, and $C_{eq} = 1.68$ μM was computed from the adsorption isotherm of dodecanol [22].

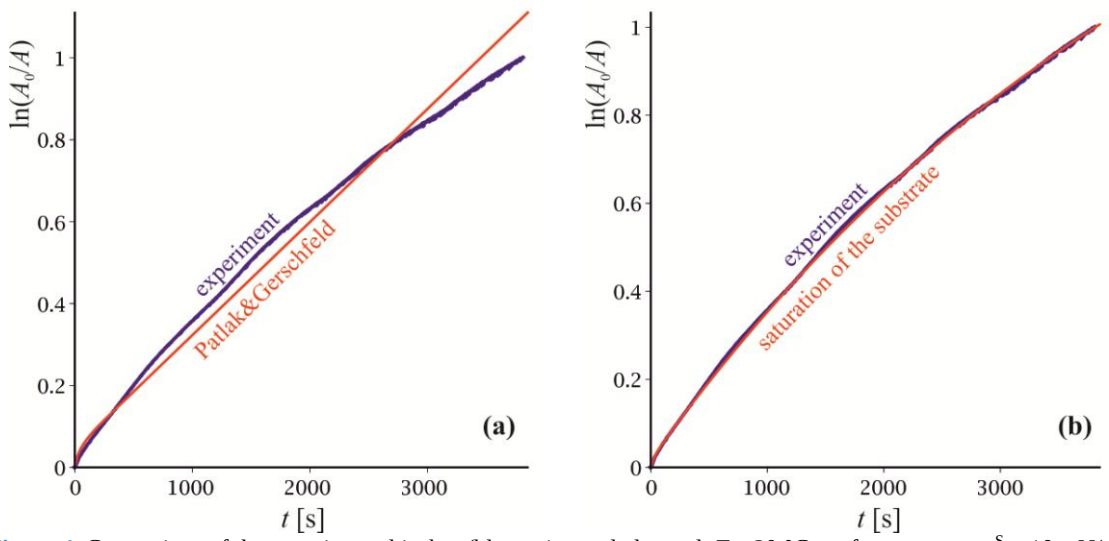

Figure 4. Comparison of the experimental isobar (blue points – dodecanol, $T = 20$ °C, surface pressure $\pi^S = 10$ mN/m, $d = 6$ mm, 2 μL dodecanol spread behind the barriers to minimize leakage) and a theoretical prediction based on a barrier-convective-diffusion regime taking into account the saturation of the substrate (red curve). The theoretical line is based on (**a**) Patlak&Gerschfeld's model (8), and **(b)** its modification (17) that takes into account the saturation of the substrate. The fitting parameters (τ_d and L_{st}) for this experiment are $\tau_d = 664$ s and $L_{st} = 0.32$ mm. The fitting parameters for all other experiments at $\pi^S = 10$ mN/m are summarized in **Table 1**.

The comparison suggests that the experiment is seemingly in consent with the saturation model at all times. Therefore, we can conclude that the aqueous substrate saturation is a significant effect at long time ($t > \tau_{sat} = L_{st} d / D \sim 10^3$ s), leading to significant curvature of the $\ln(A_0/A)$ vs. t dependence (compared to the linear dependence predicted by the original model of Patlak and Gershfeld at long times).

We performed similar experiments under a range of conditions, to determine the apparent thickness L_{st} of the stagnation layer. The results are summarized in Table 1. As a whole, they show no clear tendency with the variation in experimental conditions. The value of L_{st} is not well-reproducible, as if the "convection" is to a large extent a probabilistic phenomenon (evidenced by the significant uncertainty range), with significant variations even under seemingly equivalent conditions of the experiment.

The model was tested with a series of experimental data on different isobar surface.

Table 1. Apparent stagnated layer thickness L_{st} and characteristic time for desorption τ_d obtained from data for isobaric desorption of a spread dodecanol monolayer at $\pi^S = 10$ mN/m, $\pi^S = 15$ mN/m and $T = 20$ °C, under various conditions: different depths of aqueous substrate, mechanical stirring, directional heating, spreading of a monolayer behind the barriers of the Langmuir trough.

$\pi^S = 10$ mN/m			
***d* [mm]**	**conditions**	**L_{st} [mm]**	**τ_d [s]**
2	regular	0.40±0.07	298±176
3	regular	0.28	656
5	regular	0.37±0.12	183±122
6	regular	0.26±0.01	368±348
6	mechanical stirring	0.27±0.05	281±182

6	direct heating	0.31±0.04	393±183
6	+ 2 μL $C_{12}H_{25}OH$ behind the barriers	0.32±0.03	488±242
6	+ 5 μL $C_{12}H_{25}OH$ behind the barriers	0.41±0.10	609±52
6	+ 10 μL $C_{12}H_{25}OH$ behind the barriers	0.30±0.03	308±170
π^S = 15 mN/m			
***d* [mm]**	**conditions**	**L_{st} [mm]**	**τ_d [s]**
2	regular	0.42	244
3	regular	0.23±0.07	378±84
5	regular	0.31±0.03	250±153
6	regular	0.30±0.03	532±223
6	+ 5 μL $C_{12}H_{25}OH$ behind the barriers	0.48±0.11	257±216
6	+ 10 μL $C_{12}H_{25}OH$ behind the barriers	0.37	365
6	+ 35 μL $C_{12}H_{25}OH$ behind the barriers	0.37±0.08	0.782±140

Based on these results, we can test the four hypothesis formulated in the introduction for the source of the observed acceleration of the desorption.

(i) Convection control through aqueous substrate depth. At long times ($\sim\tau_{sat}$), we observe variations of the obtained $A(t)$ curves in line with the saturation effect, i.e. a thinner substrate saturates faster resulting in slower rate of desorption, Eq. (15). To highlight the effect we are interested in – the natural convection – we present in Figure 5 only the first minute of the measurements, where the saturation is negligible. The data shows that there is no significant influence of the aqueous substrate thickness on the velocity of desorption in the initial stage of dissolution. This excludes natural convection as a significant factor.

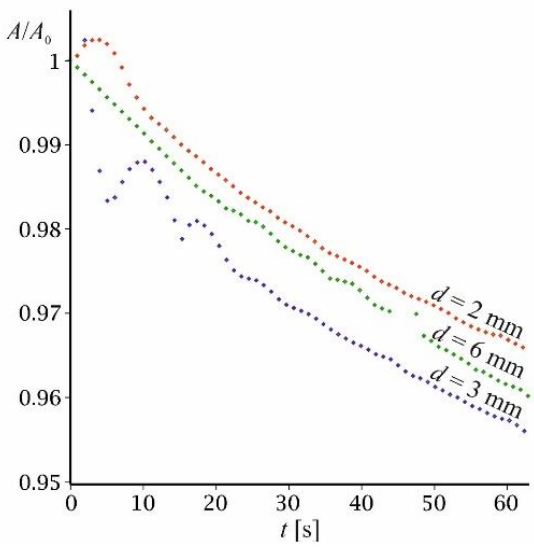

Figure 5. The independence of the isobars of the depth of the aqueous substrate at short times shows that natural convection has no significant effect on the desorption rate.

(ii) Movement of the Teflon barrier as the cause of convection. As the monolayer shrinks and the two movable barriers approach each other, the liquid surface moves relative to the bottom of the trough, which causes convection. At surface shrinking velocity of $\theta = \mathrm{d}\ln A/\mathrm{d}t$, the stagnant layer thickness is given by

$$L_{\mathrm{st}} = \left(\pi D / 2\theta\right)^{1/2} \qquad (20)$$

The equation was derived by De Keyser & Joos [25] for a trough with a different design than ours (single movable barrier instead of two moving against each other); our analysis showed that for our trough, the value of L_{st} is exactly the same. The thickness L_{st} calculated by this equation is in the range 0.7 – 2.2 mm, calculated with the experimental velocities θ (the slope of the curve in Figure 4(b)). In comparison, the values in Table 1 obtained from the fit are up to ten times lower, i.e. there must be a more significant source of apparent convection in our experiments.

(iii) Marangoni effect caused by an external temperature gradient. To test the hypothesis that Marangoni flows in the surfactant-free compartment of the trough produce significant convection, we imposed external temperature gradient on the surface by illuminating one side of the trough. Our method allows for up to four °C difference between the sides of the trough. This corresponds to surface tension difference of $\Delta\sigma = -s^{\mathrm{S}}\Delta T \sim 0.6$ mN/m, where $s^{\mathrm{S}} = 0.138\times10^{-3}$ $\mathrm{Nm^{-1}K^{-1}}$ is the surface entropy of pure water [30]. This is sufficient to cause significant Marangoni effect [31]. The result was negative – the desorption isobars are similar with and without temperature gradient, see Figure 6.

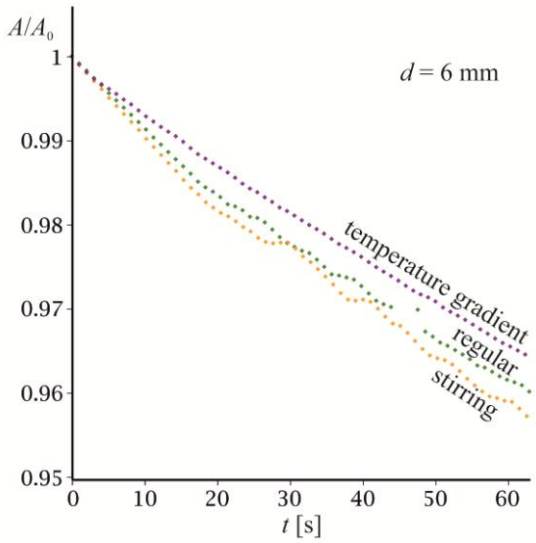

Figure 6. Dodecanol adsorption isobars under imposed temperature gradient ("temperature gradient" curve), and with mechanical stirring ("stirring" curve) of the aqueous substrate, compared to unperturbed isobar ("regular" curve).

(iv) Mechanical stirring. The clearest experimental series we made was with liquid stirring inside the trough with multiple magnetic stirrers. With appropriately chosen location of the stirrers, it turned out that the measurement of surface tension is not observably affected by the stirring, so we were able to achieve high intensity of mechanical convection. There were performed experiments at stirring speeds between 50 and 350 rpm. The average shear rate that the stirrer creates was approximately calculated by the relation apparent power/V = dissipation rate = $\eta|\nabla \boldsymbol{v}|^2$, which gives shear rate of the order of $|\nabla \boldsymbol{v}| \sim 10^3$ s^{-1}, where we assume that the apparent power is 1-2 W, the volume of the central compartment of the Langmuir trough is $V = 145\times505\times5$ mm^3 and viscosity of $\eta = 1$ mPa·s. We tried mixing with single stirrer placed in the center, and also with two stirrers placed symmetrically alongside the trough. The effect from stirring is consistently in the correct direction – it accelerates the desorption, see Figure 6. However, even for the higher stirring speed the effect on the measured isobars was small in comparison with the experimental effect shown in Figure 1 that we were trying to explain. This convinced us that convection was probably not the cause of the observed monolayer material loss, and our initial hypothesis did not stand the tests.

(v) Surfactant leakage through the movable barrier. We expect two mechanisms to lead to leakage of surfactant to the free surface behind the barrier. The *rapid transport* mechanism is via the contact between the movable barrier and the Teflon trough, where a fluid channel is present. In this case, the driving force of the transport is the difference in surface tension on the two ends of the channel, and the width of the free liquid surface between the two contacting solids controls the rate of transport. The second *slow transport* mechanism is via diffusion under the barrier (maybe with contribution from surface diffusion at the barrier|liquid interface). The driving force is in both cases the difference in chemical potential on the two sides of the movable barrier.

To test this hypothesis, we spread a monolayer in the "free" compartment of the Langmuir trough, see Figure 3, to reduce the driving force of this type of transport. This test was positive – indeed, a surfactant monolayer on the other side of the movable barrier significantly reduces the speed of material loss from the central compartment, Figure 7.

The effect is of the order of the one we previously observed, see Figure 1. The application of an increasingly dense monolayer in the free compartment leads to less and less material lost. Transport of material from the outer to the central compartment takes place for denser monolayers.

Thus, the effect of Figure 1 is not due to convection, but is caused by leakage of surfactant through the Teflon barrier. The coincidence between the theory and experiment of Figure 4 is accidental, and the values of L_{st} that we determined are an empirical measure of the rate of transport across the barrier.

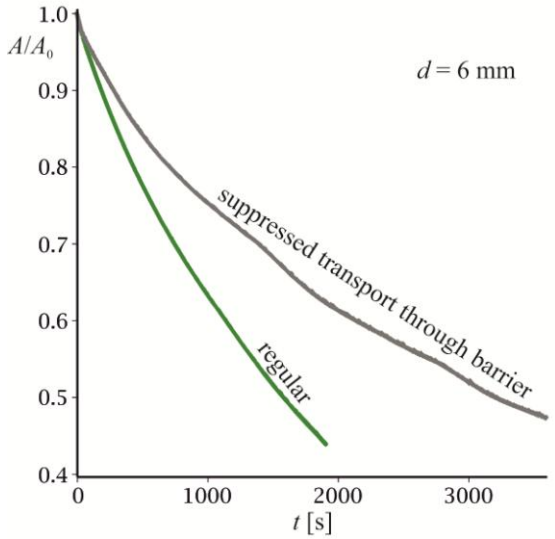

Figure 7. Effect of the suppression of the transport of surfactant through the Teflon barrier by spreading monolayer on the other side of the barrier (the experimental dots denoted as "suppressed transport through barrier"). The suppression leads to a significant decrease in rate of surfactant loss in comparison with the regular experiment with clean water surface on the other side of the barrier ("regular" curve).

To estimate the rate of leakage, we have used Eq. (22) (from Suppl. Mat.) with a single fitting parameter j_{side}. We have fixed the value of the stagnated layer thickness to $L_{st} = 0.8$ mm as given by Eq. (20) of De Keyser & Joos [25], and the characteristic time for desorption $\tau_d = 800$ s as calculated in our previous study [22]. The length of the barrier is $L_{side} = 145$ mm and the initial area of the monolayer is $A_0 = 145 \times 200$ mm^2. We have fitted only the initial stages of dissolution from 0 s to 770 s as shown in Figure 8. For longer times, the coverage of the "free" compartment becomes too high and the approximation $\Gamma_{\text{free surface}} << \Gamma$ used for the derivation of Eq. (22) is no longer valid. The obtained flux j_{side} to the outer compartment of the Teflon trough is $j_{side} = (1.2 \pm 0.1) \times 10^{-10}$ mol·s^{-1}·m^{-1}. As can be seen from Figure 8, at $t \sim 770$ s the initial monolayer surface has decreased by 28% (blue curve at Figure 8). The decrease of the area due to the monolayer dissolution is 12% (green curve at Figure 8). The rest (16%) is because of the surfactant passing behind the barriers.

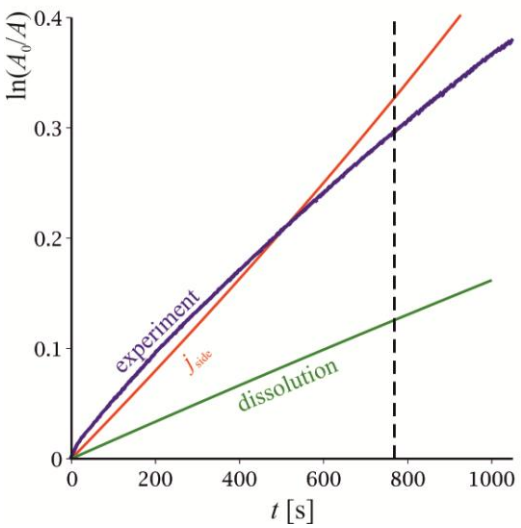

Figure 8. Comparison of the experimental isobar (blue curve – dodecanol, $T = 20$ °C, surface pressure $\pi^S = 10$ mN/m, $d = 6$ mm) and a theoretical prediction based on Eq. (22) (red curve) to about $t \sim 770$ s that takes into account the leakage through the barriers. The green curve represents the monolayer dissolution in accordance with Eq. (22) with $j_{side} = 0$.

5. Conclusion

With regards to our hypothesis that the observed acceleration of the desorption of a sparingly soluble monolayer is due to convection [22], the result from this study is negative: we showed that convection in the bulk of the Langmuir trough has a relatively small influence on the rate of desorption. The leakage through the movable barrier was shown to be responsible for the effect in question. The apparent values of the stagnated layer thickness L_{st} in Table 1 are, therefore, a measure of the rate of leakage.

We made attempts to control the leakage by choose appropriate surface density of the monolayer at the outer side of the movable barrier. This approach indeed slows down the leakage, but is difficult to control and the outcome was overall not satisfactory. We also tried to place dodecanol crystals behind the barriers, but this led to transport of surfactant in the opposite direction – from the outer to the central part of the trough, where the surface tension is kept constant.

We also attempted monitoring for leaks and disregarding runs where leaks were detected, similar to Hills [32]. This strategy seems to work at lower temperatures [22], where leakage appears only in a fraction of the experiments in a stochastic manner. At increased temperature, however, the approach no longer works since the leakage appears to be of relatively well defined rate (probably due to a transition from transport via the meniscus between the movable barrier and the Teflon trough to transport via solid surface diffusion under the barrier). Another difficulty with Hills' approach is that with the surfactants we study even relatively dense layers have negligibly low surface pressure.

Other approaches to limit the leakage exist in the literature. One measure against it is changing appropriately the material of the movable barrier [35, 36]. Other approaches include spring-loading of the barriers against the trough well [37] and using metal reinforcement bar along the top of the plastic barrier [34].

The results of our work mean that the desorption constant values that we have determined in Ref. [22] are overestimated and the time for desorption τ_d is underestimated, i.e. the barrier energy must be even more significant.

Acknowledgements

The work is funded by National Science Fund through Contract No. 80-10-140 from 15.04.2019 with Sofia University.

The authors are very thankful to Prof. Veselin Petrov and Prof. Lyudmil Lyutov from Sofia University "St. Kliment Ohridski" and Albert Varonov from Bulgarian Academy of Sciences for the fruitful discussions and some data evaluations.

6. References

1. *Emulsions and Emulsion Stability: Surfactant Science Series/61*, Ed. Johan Sjoblom, CRC Press; 2nd ed. (2005).
2. *Emulsion Formation and Stability*, Ed. Prof. Dr. Tharwat F. Tadros, Wiley press (2013).
3. *Nanoemulsions: Formulation, Applications, and Characterization*, Ed. Seid Mahdi Jafari and David Julian McClements, Elsevier (2018).
4. V.S. Sastri, *Corrosion Inhibitors. Principles and Applications*, Wiley, 1st ed. (1998).
5. Mumtaz A. Quraishi, Dheeraj S. Chauhan and Viswanathan S. Saji, *Heterocyclic Organic Corrosion Inhibitors. Principles and Applications*, Elsevier (2020).
6. R. Miller and K. Lunkenheimer, *Colloid Polym. Sci.*, 1986, **264**, 357–361. https://doi.org/10.1007/BF01418196.
7. J. Eastoe and J. S. Dalton, Adv. *Colloid Interface Sci.*, 2000, **85**, 103–144. https://doi.org/10.1016/S0001-8686(99)00017-2.
8. S. Dukhin, G. Kretzschmar and R. Miller, *Dynamics of adsorption at liquid interfaces, Theory, experiment, application*, Elsevier, Amsterdam (1995).
9. R. Miller, E. V. Aksenenko and V. B. Fainerman, *Adv. Colloid Interface Sci.*, 2017, **247**, 115–129. https://doi.org/10.1016/j.cis.2016.12.007.
10. S.-Y. Lin, K. McKeigue and C. Maldarelli, *AIChE J.*, 1990, **36**, 1785–1795. https://doi.org/10.1002/aic.690361202.
11. D. O. Johnson and K. J. Stebe, *J. Colloid Interface Sci.*, 1996, **182**, 526–538. https://doi.org/10.1006/jcis.1996.0497.
12. R. Miller, A. V. Makievski and V. B. Fainerman, in *Surfactants – chemistry, interfacial properties, applications*, ed. V. B. Fainerman, D. Möbius and R. Miller, Elsevier (2001), ch. 4.
13. J. T. Davies and E. Rideal, *Interfacial phenomena*, Academic Press, (1963). ch. 4.
14. W. Adamson and A. P. Gast, *Physical chemistry of surfaces*, Wiley, 6th ed., (1997), Sec. IV-7.

15. MacRitchie, *J. Colloid Interface Sci.*, 1985, **105**, 119–123. https://doi.org/10.1016/0021-9797(85)90353-4.
16. R. D. Smith and J. C. Berg, *J. Colloid Interface Sci.*, 1980, **74**, 273–286. https://doi.org/10.1016/0021-9797(80)90190-3.
17. D. Vollhardt and U. Retter, *J. Phys. Chem.*, 1991, **95**, 3723–3727. https://doi.org/10.1021/j100162a052.
18. T. V. Peshkova, I. L. Minkov, R. Tsekov and R. I. Slavchov, *Langmuir*, 2016, **32**, 8858–8871. https://doi.org/10.1021/acs.langmuir.6b02349.
19. J. P. Slotte and S. Illman, *Langmuir*, 1996, **12**, 5664–5668. https://doi.org/10.1021/la960401l.
20. D. S. Dimitrov, I. I. Panaiotov, P. Richmond, L. Ter-Minassian-Saraga, *J. Colloid Interface Sci.*, 1978, **65**(3), 483-494. https://doi.org/10.1016/0021-9797(78)90100-5.
21. A. G. Bois, I. I. Panaiotov, J. F. Baret, *Chemistry and Physics of Lipids*, 1984, **34**(3), 265-277.
22. I. L. Minkov, D. Arabadzhieva, I. Salama, E. Mileva, R. I. Slavchov, *Soft Matter*, 2019, **15**, 1730-1746. https://doi.org/10.1039/C8SM02076K.
23. L. Ter Minassian-Saraga, *J. Chim. Phys.*, 1955, **52**, 181–200. https://doi.org/10.1051/jcp/1955520181.
24. L. Ter Minassian-Saraga, *J. Colloid Sci.*, 1956, **11**, 398–418. https://doi.org/10.1016/0095-8522(56)90157-X.
25. P. De Keyser and P. Joos, *J. Colloid Interface Sci.*, 1983, **91**, 131–137. https://doi.org/10.1016/0021-9797(83)90320-X.
26. J. F. Baret, A. G. Bois, L. Casalta, J. J. Dupin, J. L. Firpo, J. Gonella, J. P. Melinon and J. L. Rodeau, *J. Colloid Interface Sci.*, 1975, **53**, 50–60. https://doi.org/10.1016/0021-9797(75)90034-X.
27. C. S. Patlak and N. L. Gershfeld, *J. Colloid Interface Sci.*, 1967, **25**, 503-513. https://doi.org/10.1016/0021-9797(67)90061-6.
28. R. I. Slavchov, I. L. Minkov, D. Arabadzieva and E. Mileva, *Nanoscience & Nanotechnology*, 2018, **18**(1) 21-33. ISSN: 1313-8995.
29. S. R. De Groot, P. Mazur, *Non-equilibrium Thermodynamics*, Dover Publications, Inc. New York (1984).
30. S. R. Palit, *Nature* , 1956, **177**, 1180–1180. https://doi.org/10.1038/1771180a0.
31. J. K. Novev, N. Panchev, R. I. Slavchov, *Chemical Engineering Science*, 2017, **171**, 520–533. https://doi.org/10.1016/j.ces.2017.06.016.
32. B. A. Hills, *J. Physiol.*, 1985, **359**, 65-79. https://doi.org/10.1113/jphysiol.1985.sp015575.
33. S. Schürch, H. Bachofen, J. Goerke, F. Green, *Biochim. Biophys. Acta Biomembr.*, 1992, **1103**(1), 127-136. https://doi.org/10.1016/0005-2736(92)90066-U.
34. F. Grunfeld, *Rev. Scientific. Inst.*, 1993, **64**, 548 – 555. https://doi.org/10.1063/1.1144231.
35. G. Ma and H. C. Allen, *Langmuir*, 2007, **23**, 589-597. https://doi.org/10.1021/la061870i.

36. N. J. Hardy, T. H. Richardson, F. Grunfeld, *Colloids Surf. A Physicochem. Eng. Asp.*, 2006, **284-285**, 202-206. https://doi.org/10.1016/j.colsurfa.2006.02.001.
37. M. M. Lipp, K. Y. C. Lee, J. A. Zasadzinski, A. J. Waring, *Rev. Sci. Instrum.*, 1997, **68**(6), 2574-2582. https://doi.org/10.1063/1.1148163.

Supplement A: list of symbols

A area covered by the monolayer

A_0 area covered by the monolayer in the initial moment

C bulk concentration of the surfactant

$C(z = 0, t)$ bulk subsurface surfactant concentration (right next to the surface)

C_{eq} bulk equilibrium surfactant concentration with respect to monolayer

C_∞ unperturbed bulk concentration of the surfactant

D diffusion coefficient of the surfactant

L_{side} length of the Teflon barrier

L_{st} thickness of the stagnated layer

T absolute temperature

d depth of the Langmuir trough

j^S rate of the (monolayer)→(subsurface) barrier process of desorption, $j^S = v_d - v_a$

j^S_∞ surface flux at stationary state

j_{side} flux of surfactant due to leakage through the barriers

k_d rate constant for desorption, $v_d = k_d C_{eq}$

n amount of dodecanol in the monolayer [mol]

n_0 total amount of dodecanol in the system [mol]

t time

v_a adsorption rate, $v_a = k_d C(z = 0)$

v_d desorption rate, $v_d = k_d C_{eq}$

z cartesian coordinate normal to the surface

Γ adsorption of the surfactant

$\Gamma_{free\ surface}$ adsorption of the surfactant in the "free" compartment behind the Teflon barriers

π^S surface pressure, $\pi^S = \sigma_0 - \sigma$

σ surface tension

σ_0 surface tension of the neat surface of the solution

$\tau_d = \Gamma/k_d C_{eq}$ characteristic time for desorption

$\tau_{sat} = L_{st} d/D$ characteristic time for saturation of the trough volume with surfactant

$\tau_{st} = L_{st}^2/D$ characteristic time for transition from barrier/diffusion to barrier/convective diffusion regime

$\tau_{tr} = D/k_d^2$ characteristic time for transition from barrier to diffusion controlled regime

Supplement B: surface area $A(t)$

The solution of Eq. (18) with j^S from Eq. (17) is

$$\ln\frac{A_0}{A}=\frac{L_{st}C_{eq}}{\Gamma}\left[\frac{d}{L_{st}}\left(1-e^{-\frac{M}{1+M}\frac{t}{\tau_{sat}}}\right)+2M^2\sum_{n=1}^{\infty}\frac{1-e^{-m_n^2\frac{t}{\tau_{st}}}e^{-\frac{M}{1+M}\frac{t}{\tau_{sat}}}}{\left(m_n^2+\frac{M}{1+M}\frac{L_{st}}{d}\right)\left(M+M^2+m_n^2\right)}\right]. \quad (21)$$

We applied this expression to fit the experimental data for the isobars at different conditions.

The integrated Eq. (19) that takes into account the leakage behind the barriers is

$$\ln\frac{A_0}{A}=\ln A_0-\frac{C_{eq}d}{\Gamma}e^{-\frac{M}{1+M}\frac{t}{\tau_{sat}}} -\ln\left[A_0e^{-\frac{C_{eq}d}{\Gamma}}+\frac{2L_{st}L_{side}j_{side}d}{\Gamma D}\frac{1+M}{M}\left(\mathrm{Ei}\left(1,\frac{C_{eq}d}{\Gamma}\right)-\mathrm{Ei}\left(1,\frac{C_{eq}d}{\Gamma}e^{-\frac{M}{1+M}\frac{t}{\tau_{sat}}}\right)\right)\right]. \quad (22)$$